Biosensors and Bioelectronics 66 (2015) 596–602

Contents lists available at ScienceDirect

Biosensors and Bioelectronics

journal homepage: www.elsevier.com/locate/bios

A competitive photoelectrochemical assay for estradiol based on in situ generated CdS-enhanced TiO_2

Rongxia Li [a], Yixin Liu [b], Tao Yan [b], Yueyun Li [b], Wei Cao [b], Qin Wei [b], Bin Du [a,*]

[a] School of Resources and Environment, University of Jinan, Jinan 250022, PR China
[b] Key Laboratory of Chemical Sensing & Analysis in Universities of Shandong (University of Jinan), School of Chemistry and Chemical Engineering, University of Jinan, Jinan 250022, PR China

ARTICLE INFO

Article history:
Received 3 October 2014
Received in revised form
23 November 2014
Accepted 1 December 2014
Available online 3 December 2014

Keywords:
Photoelectrochemical
Competitive bioassay
In situ
Small molecules

ABSTRACT

A novel and simple photoelectrochemical (PEC) bioassay protocol for estradiol was proposed based on in situ generated CdS-enhanced TiO_2 film via competitive strategy. The CdS was generated in situ by immediately dropping S^{2-} onto the Cd^{2+}-functionalized titanium phosphate nanoparticles (TiP@Cd^{2+}). The TiO_2 photoactive sensing film with countless active sites was obtained by calcination and further explored for estradiol (E_2) capture. The TiP@Cd^{2+} was used as labels and immobilized through affinity-specific binding with E_2 on the surface of the electrode. Greatly enhanced sensitivity was achieved by using porous TiP nanoparticles as carriers to load a large amount of Cd^{2+} and further for more CdS production through the S^{2-} deposition. What's more, the photocurrent of CdS generated on the electrode surface could be significantly amplified by the coupling of CdS and TiO_2, which could enhance the excitation and photo-to-electric conversion efficiency. Through the application of a competitive binding assay, the proposed biosensor showed high sensitivity with a detection limit down to 2 pg/mL. This simple and fast PEC E_2-sensing approach offers great promise to extend its application for the assay of small molecules of biomedical, food and environmental interest. Additionally, the strategy of employing in situ generated narrow-band gap semiconductors paves a new way for PEC sensing.

1. Introduction

Quality in life is an ever growing interest all around the world. The quality of life is governed by several factors such as control of diseases, drug development, environment cleaning, food safety and homeland security. Estradiol (E_2), as endocrine disruptor chemical with estrogenic activity, can bind to the estrogen receptor in the body and potentially alter the normal physiological function of the endocrine systems (Hintemann et al., 2006, Tanaka et al., 2004, Wen et al., 2006). Presence of low concentration of estrogens in the environment can cause abnormal sexual development of animals and decrease the average numbers of human spermatozoa (Chang et al., 2009). Therefore, rapid detection, quantification of E_2 in aquatic environments is a crucial task to protect the health of human and animals. Photoelectrochemical (PEC) detection is a newly emerging but dynamically developing analytical technique that is expected to have the advantages of both fluorescence and electrochemical sensors (Dong et al., 2004, Gill et al., 2008, Haddour et al., 2006, Ikeda et al., 2009, Liang and Guo, 2007, Liang et al., 2006, Pardo-Yissar et al., 2003). In PEC detection, due to the separation of excitation source and detection signal, the sensitivity is potentially high (Wang et al., 2009b). Compared to a single semiconductor as the photoactive material, semiconductor heterojunctions are considered to help in promoting the separation of photo-generated charge carriers (Shi, 2012). In order to extend the photoresponse of a wide-bandgap semiconductor and thus improve the energy conversion efficiency, many visible-light-responsive or narrow-bandgap semiconductors have been utilized in PEC sensing, such as chalcogenide quantum dots, ruthenium polypyridyl sensitizers, porphyrins, phthalocyanine, polypyrrole, polyaniline or poly-(3-hexylthiophene) (Chen et al., 2012, Li et al., 2011, 2013, Liang et al., 2011, Ma et al., 2013, Sun et al., 2013, Tu et al., 2010, Zhang et al., 2012, Zhao et al., 2012a, 2012b, 2012c). All of them need to be prepared in advance before being applied in PEC sensing. Recently, a PEC aptasensing strategy for Ag^{+} based on in situ generated AgBr-enhanced ZnO nanorod has been reported (Li et al., 2014). Inspired by this thought, a novel competitive biosensor for E_2 was proposed based on the in situ generated CdS via dipping S^{2-} on the electrode surface.

As a kind of PEC semiconductor materials, TiO_2 have gained much attention in PEC sensors in recent years (Li et al., 2011, Lu

* Corresponding author. Fax: +86 531 82765730.
E-mail address: dubin61@gmail.com (B. Du).

http://dx.doi.org/10.1016/j.bios.2014.12.002
0956-5663/

et al., 2013, Tu et al., 2010, Wang et al., 2009a). However, bare TiO_2 is photoelectrochemically active only under UV irradiation, and the photo holes formed by illuminating are very powerful oxidizers ($E=+3.1$ V versus NHE) (Hoffmann et al., 1995) due to its wide band gap. Both of them limited its application in PEC biosensing. As we all know, CdS is one of the most widely studied semiconductors as a photoanode. Also the CdS nanoparticles have been successfully used for PEC sensors (Pardo-Yissar et al., 2003, Qian et al., 2010, Wang et al., 2009c, Zhao et al., 2011, 2012b). After CdS absorb photons with energy higher than the band gap, electrons are emitted from the valence band to the conduction band, producing the electron–hole pairs and further generating photocurrent. However, the photo-to-current conversion efficiency of CdS nanoparticles was low due to the electron–hole recombination (Hosokawa et al., 1996). For the application in PEC sensing, a system with enhanced photocurrent intensity and less electron–hole recombination will be desirable. Coupling of small and gap semiconductors with large band gap ones to facilitate charge separation is an efficient way to improve the photocurrent (Borgarello et al., 1985, Sant and Kamat, 2002, Tambwekar et al., 1999). The coupling of CdS and TiO_2 film would result in enhanced photoelectric conversion efficiency by means of the extended visible light response, the fast separation of charge carriers and the light scattering in the film arrays (Baker and Kamat, 2009, Kim et al., 2011, Sant and Kamat, 2002, Shalom et al., 2009, Wang et al., 2009b', 2006).

In this work, E_2 and anti-E_2 were adopted as a model system to evaluate the sensing ability of TiP@Cd^{2+}–anti-E_2 conjugates as a competitive reagent. Herein, a novel PEC biosensor was proposed for the assay of E_2 based on the in situ generated CdS-enhanced TiO_2film-based photoelectrochemistry via a competitive binding protocol. A TiO_2 photoelectroactive film was first deposited onto the ITO electrode. Following which, a constant concentration of E_2 was immobilized on the TiO_2 film, and then the TiP@Cd^{2+} loaded anti-E_2 was assembled onto the electrode via specific immunoreaction of antigen–antibody. Afterwards, Na_2S was dropped on the TiP@Cd^{2+}–anti-E_2 modified electrode for the in situ generation of CdS. The fabricated PEC biosensor for E_2 showed good performances with a rapid response, simple operation, high sensitivity and good selectivity. This assay was also applied to the localized lake water and the results were satisfactory. More importantly, the strategy of employing in situ generated narrow-bandgap semiconductors to enhance the photocurrent opens an alternative horizon for PEC sensing.

2. Materials and methods

2.1. Materials and reagents

Indium tin oxide (ITO, resistivity 10 Ω/sq) is obtained from Zhuhai Kaivo Electronic Components Co. Ltd., China. ITO slices were sonicated in acetone, ethanol and distilled water respectively, for about 30 min each, and then dried under the flow of nitrogen. Tetrabutyl titanate (TBOT), sodium dodecyl sulfate (SDS), cadmium nitrate tetrahydrate ($Cd(NO_3)_2\cdot 4H_2O$), poly (allylamine hydrochloride) (PAH), Sodium sulfide (Na_2S) and phosphoric acid (H_3PO_4) were from Shanghai Chemical Reagent Co., Ltd. (Shanghai, China). Estradiol (E_2) and anti-estradiol (anti-E_2) were purchased from Beijing Biosynthesis Biotechnology Co., Ltd. (Beijing, China). Bovine serum albumin (BSA) and ascorbic acid (AA) were from Sigma-Aldrich. Phosphate buffer saline (PBS) with different pH values were prepared by mixing the stock solution of 0.1 M of NaH_2PO_4 and Na_2HPO_4. All other reagents were of analytical reagent grade and used without further purification. Ultrapure water obtained from a Millipore water purification system (Molsheim, France) was used in all run.

2.1.1. Apparatus

Scanning electron microscope (SEM) images and Energy Dispersive X-Ray Spectroscopy (EDS) were recorded by JEOL JSM-6700F microscope (Japan). Fourier transform infrared (FTIR) spectrum was obtained with a Perkin-Elmer 580B spectrophotometer (Perkin-Elmer, United States). Photocurrent was measured by the current–time curve experimental technique on an electrochemical workstation (Zahner Zennium PP211, Germany) at a bias voltage of 0.1 V following a 200 W LED excitation. The distance between the light source and the electrode was fixed at 10 cm. All experiments were carried out at room temperature using a conventional three electrode system with a modified ITO as the working electrode, a platinum wire as the auxiliary electrode, and a standard calomel electrode as the reference electrode.

2.2. The synthesis of TiO_2

TiO_2 was synthesized according to the previous report with slight modification (Huang et al., 2013). 0.02 mol of tetrabutyl orthotitanate (TBOT) was dissolved into 30 mL of ethanol and stirred for 120 min, and then the suspension was transferred to a 50 mL teflon-lined autoclave and maintained at 200 °C for 10 h. The obtained white precipitates were collected and washed thoroughly with distilled water and absolute ethanol for several cycles and then dried in vacuum at 80 °C for 12 h.

2.3. The preparation of TiP@Cd^{2+} and TiP@Cd^{2+}–anti-E_2 conjugates

The TiP@Cd^{2+} was synthesized according to the previous report (Feng et al., 2012). Briefly, TiP nanoparticles were synthesized by using SDS as the structure-directing agent, and tetrabutyl titanate (TBOT) as the titanium source (details in the Supporting material). For the synthesis of metal-ion functionalized titanium phosphate (TiP@Cd^{2+}), first, 1 mL of TiP nanoparticles (40 mg/mL) was dispersed in 17 mL of 10 mM $Cd(NO_3)_2$ $4H_2O$ aqueous solution and stirred at 50 °C for 24 h. Then, the resulted hybrid nanoparticles were obtained by centrifugation and rinsed with water for several times.

To fabricate TiP@Cd^{2+}–anti-E_2 bioconjugates, TiP@Cd^{2+} hybrid was dispersed in 7.5 mL of PAH (2 mg/mL) aqueous solution and stirred for 1 h. Then, the hybrid was centrifuged and washed with water, then dispersed in 2 mL of glutaraldehyde (wt. 2.5%) and shaked for 2 h, followed by centrifuging and washing. Subsequently, the hybrid was added into 100 μL of anti-E_2 (1 mg/mL) solution and shaked for 2 h to obtain TiP@Cd^{2+}–anti-E_2 bioconjugates. Centrifugation was carried out to remove the free anti-E_2, and then the TiP@Cd^{2+}–anti-E_2 conjugates was dispersed in 2 mL of PBS (pH 7.4) containing 1% BSA and stored in 4 °C until use.

2.4. Construction of the competitive PEC sensing platform and in situ CdS generated detection

The precleaned ITO surface was modified with 5 μL of TiO_2 solution (3 mg/mL) and dried at room temperature, then the modified electrodes were annealed to ensure particles adhesion to the substrate stably at 400 °C for 2 h in air (recorded as TiO_2/ITO). The annealed electrode surface was incubated with 5 μL of E_2 for 1 h at 4 °C (recorded as E_2/TiO_2/ITO). For the competition binding assay, first, TiP@Cd^{2+}–anti-E_2 conjugates solution was mixed with different concentrations of E_2 for 50 min. Then, after using BSA (1%) to block the nonspecific binding sites of the electrodes, 5 μL of the mixing solution of TiP@Cd^{2+}–anti-E_2 and E_2 was dropped onto electrode surface and incubated for another 50 min to facilitate the competitive immunoassay. After each step in the above modification, the modified ITO electrode was washed with PBS, and

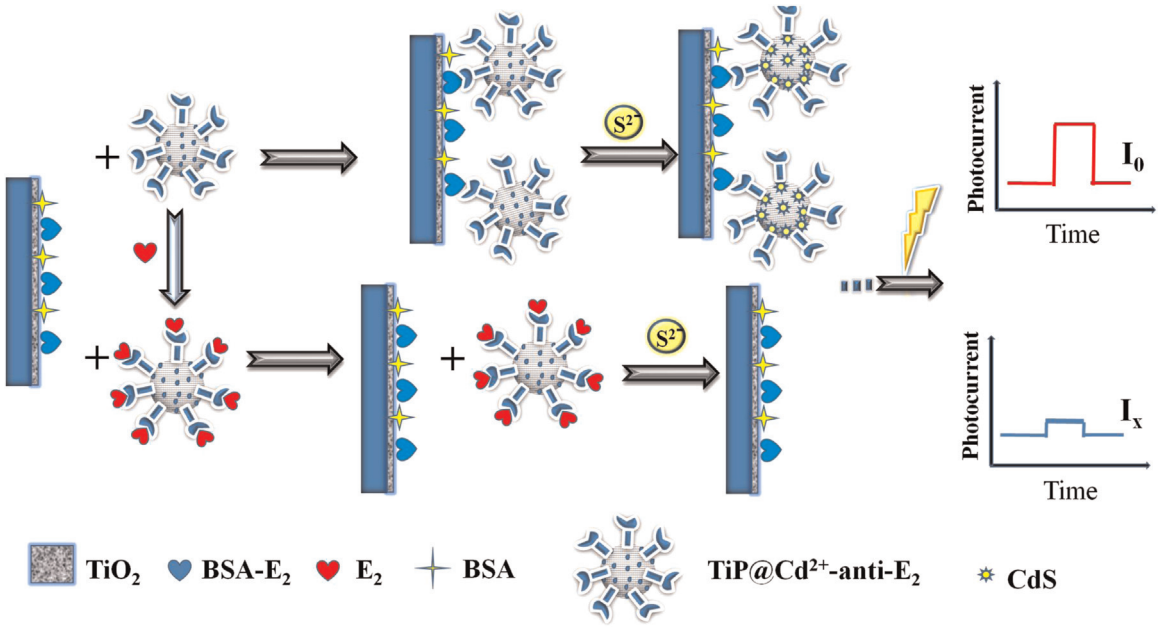

Scheme 1. Schematic diagram of the immunosensor construction process .

dried at room temperature. Then in situ generated CdS-enhanced photocurrent was carried out, typically, 5 μL of Na_2S solution (0.7 M) was dropped and incubated for 30 min at room temperature in the dark. After rinsed with copious water, the fabricated PEC sensor was applied to detect E_2 in PBS (pH 7.0, 0.1 M) containing 0.1 M AA by current–time curve experimental

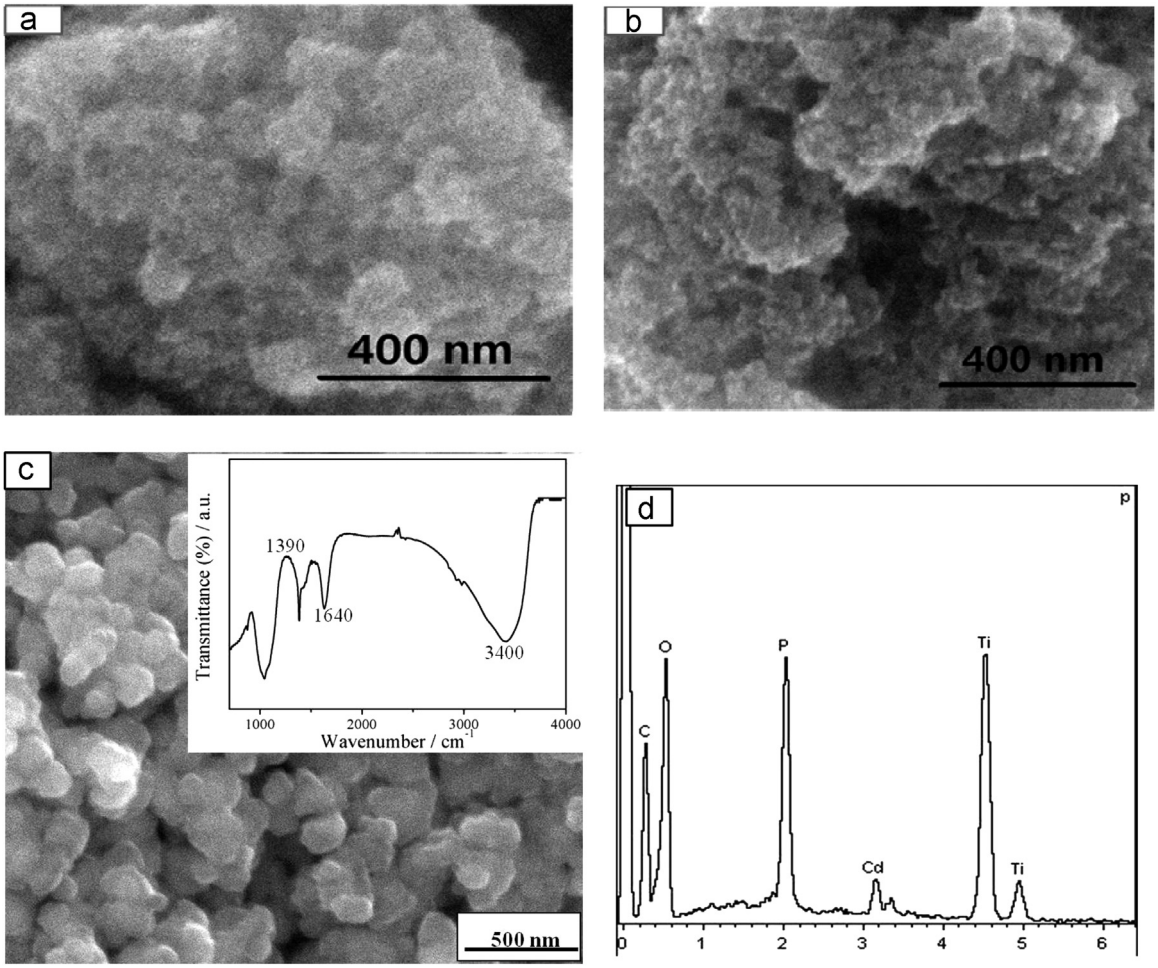

Fig. 1. The SEM images of TiO_2 immobilized ITO before (a) and after (b) calcinations; (c) the SEM images of TiP@Cd^{2+}, the inset: FT-IR spectra of TiP; (d) EDS spectra of TiP@Cd^{2+}.

technique at the bias voltage of 0.1 V following the 200 W LED light excitation. The fabrication process of the proposed immunosensor is shown in Scheme 1. And the stepwise modification of the electrode was characterized by electrochemical impedance spectra (EIS) and photocurrent–time curve technique, details in the Supporting material.

3. Results and discussion

3.1. Characterization of the materials

In this work, the ITO modified with TiO_2 was calcined firstly for the following modification. According to the SEM images in Fig.1, compared with the one without calcinations (a), there exits obviously uneven porous structure on the surface of calcined ITO modified with TiO_2 (b). The uneven structure could not only facilitate the separation of photoinduced electron-holes, but also provide larger surface area for the following loading of E_2, thus decrease the background signal.

As shown from the SEM images of TiP@Cd^{2+} in Fig. 1c, the as-synthesized TiP nanoparticles have an average size of about 55 nm. According to the N_2 adsorption–desorption isotherms (Fig. S1 ESI), the BET surface area of the TiP nanoparticles was 48.52 nm with open nanoporous structures, which makes it attractive for Cd^{2+} sorption purposes, and also facilitates the ion-exchange process (Feng et al., 2012) made the as-prepared TiP material. According to the FT-IR spectrum (the inset of Fig. 1c), the main peaks at ~1390, 1650 and 3400 cm^{-1} suggested that hydroxyl (OH), carboxyl (COOH) and carbonyl (> C=O) present on the TiP. These oxygen-containing functional groups present abundantly on the external and internal surfaces of TiP pores, which can provide numerous chemical sorption sites and thereby increase the sorption capacity of TiP. The incorporation of Cd^{2+} into the TiP nanoparticles was also confirmed by EDS (Fig. 1d), in which Cd peaks was clearly observed.

3.2. Characterization of the in situ generated CdS films

The UV–vis diffuse reflectance spectra of TiO_2 (a), TiO_2/TiP–CdS (b), and CdS (c) are presented in Fig. 2A. With the dropping of S^{2-},

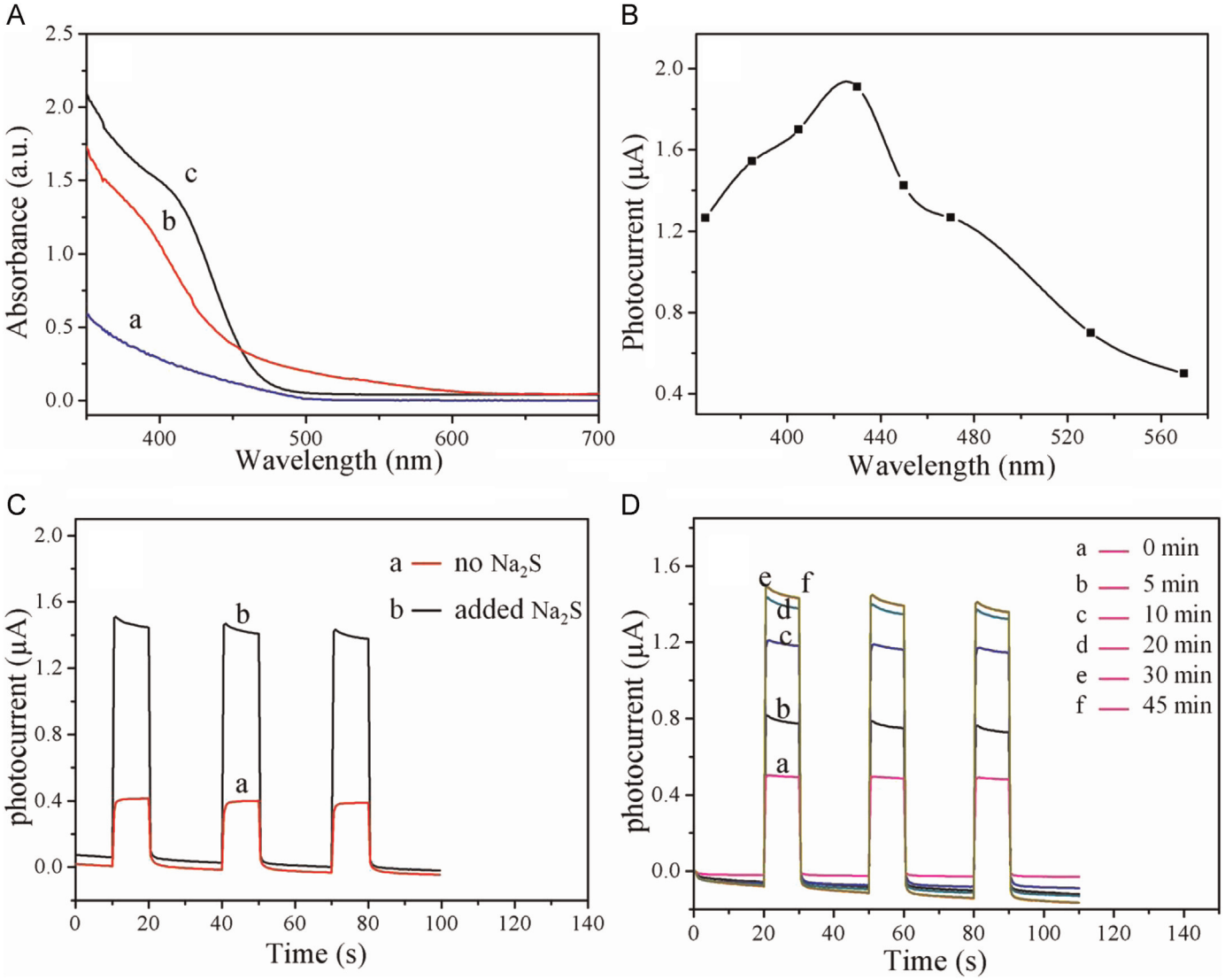

Fig. 2. (A) UV–vis diffuse reflectance spectra of TiO_2 (a), TiP–CdS (b), and CdS (c). The spectra were referenced to ITO film. (B) Photocurrent action spectrum of the in situ generated CdS on the TiP@Cd^{2+}–anti-E_2/E_2/TiO_2/ITO electrode. (C) Photocurrent of TiP@Cd^{2+}–anti-E_2/E_2/TiO_2/ITO electrode before (a) and after (b) the addition of Na_2S (0.7 M). (D) Photocurrent of the Na_2S dropped TiP@Cd^{2+}–anti-E_2/E_2/TiO_2/ITO electrode for different times. Photocurrent–time curves were recorded at a bias voltage of 0.1 V in PBS (0.1 M, pH 7.0) that contained 0.1 M AA.

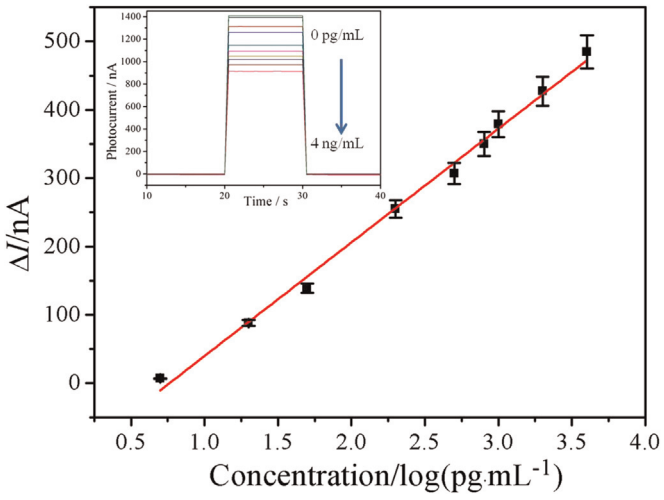

Fig. 3. Calibration curves for estradiol in the concentration of 5.0 pg/mL~4 ng/mL. $\Delta I = I_0 - I_n$, I_n is the photocurrent of the PEC sensor to a series of different concentrations of estradiol, I_0 is the photocurrent of the PEC sensor to the blank sample containing no estradiol. (inset: the photocurrent of the PEC sensor to a series of different concentrations of 0.005 ng/mL, 0.02 ng/mL, 0.05 ng/mL, 0.2 ng/mL, 0.5 ng/mL, 0.8 ng/mL, 1 ng/mL, 2 ng/mL and 4 ng/mL).

reached a peak value at ~430 nm, indicating that the photocurrent originates mainly from the excitation of the in situ generated CdS. In the subsequent experiments, 430 nm was chosen as the optimal excitation wavelength. Based on the absorption spectra, photocurrent action spectrum, and the use of AA as a hole scavenger, the resulting photocurrent can be attributed to the injection of the photogenerated electrons of CdS into the conduction band of TiO_2 and then into the ITO electrode.

As shown in Fig. 2C, compared with the photocurrent response when the absence of Na_2S (curve a), a remarkable enhancement of almost 3 times higher of the photocurrent was observed after the adding of Na_2S (curve b), which further testify the change of photocurrent response was ascribed to the generation of CdS. When the Na_2S dropped on the ITO/TiO_2/E_2/TiP@Cd^{2+}–E_2 electrode, the photocurrent increased as the reaction time increased (Fig. 2D). This is because, as the dipping time increased, the particle size and the amount of the generated CdS gradually increased, and thus the photocurrent increased (curves a–f, Fig. 2D). The photocurrent gradually increased as the dipping time increased from 5 to 30 min. However, with a further increase in dipping time from 30 to 45 min, the absorption spectra changed little (curves f and g, Fig. 2D), suggesting that no more CdS nanocrystals grew on the TiO_2 surface. In summary, these data

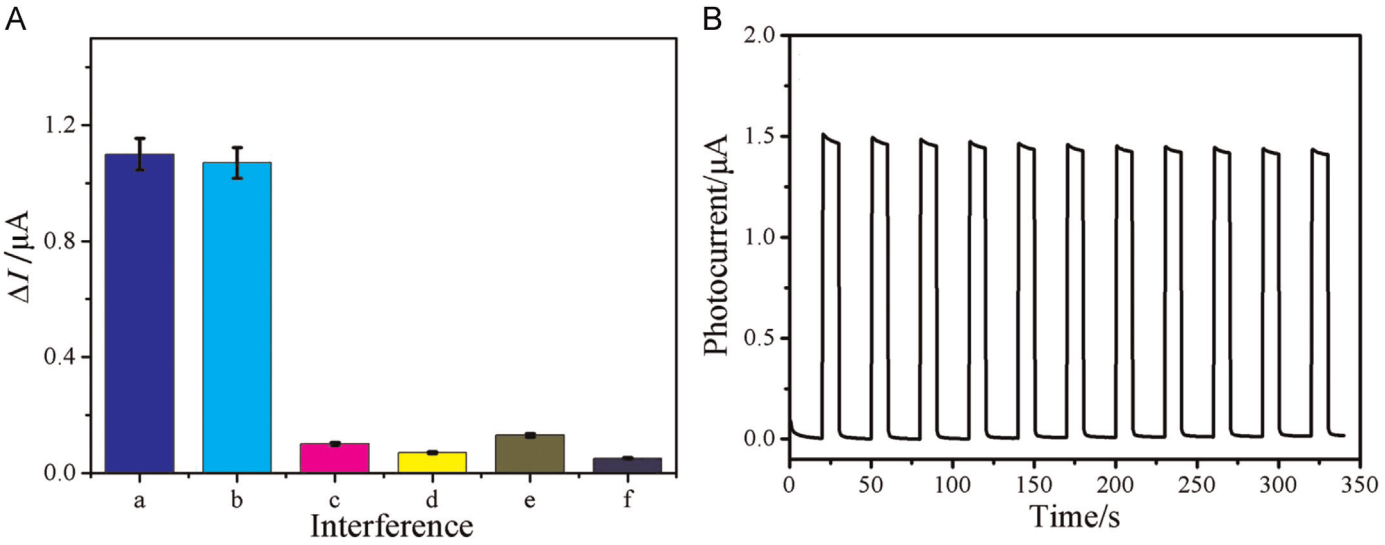

Fig. 4. (A) The selectivity of the immunosensors: (a) estradiol (1 ng/mL), (c) 4-nnonylphenol (100 ng/mL), (d) estriol (100 ng/mL), (e) 1-aminoanthraquinone (100 ng/mL), (f) 2-methoxynaphthalene (100 ng/mL) and mixture of estradiol (1 ng/mL) and 100-fold interference (b); (B) time based photocurrent response of the PEC electrode with irradiation (430 nm) repeated every 10 s under several on/off irradiation cycles for 300 s.

Table 1
Detection results of estradiol-spiked wastewater effluent samples.

Sample no.	The added content (pg/mL)	The detected content (pg/mL)	The average value of detected content (pg/mL)	RSD (%)	Recovery (%)
1	5	5.28, 5.39, 5.18, 5.35, 5.42	5.324	1.8	106.5
2	10	10.86, 10.45, 10,67, 11.08, 10.98	10.808	2.33	108.1
3	20	21.05, 20.97, 20.83, 21.26, 21.58	21.138	2.74	104.7

the absorption spectra exhibited an obvious enhancement in the visible wavelength range (b), especially the pronounced enhancement in the range of ~450 nm and lower, which corresponding to the UV–vis spectra of CdS (c). This result agrees the light-absorption property of CdS reported by another group (Shen et al., 2011). Fig. 2B shows the photocurrent action spectrum of an ITO/TiO_2/TiP@Cd^{2+}–CdS electrode in the presence of AA as a sacrificial electron donor. The photocurrent closely follows the absorbance spectrum of CdS nanoparticles as shown in Fig. 2A, and it confirmed the successful assembly of CdS on the surface of PEC sensor.

3.3. Optimization of the detection conditions

In order to obtain high and stable photocurrent of CdS, electron donors are necessary. In this work, AA was used as an electron donor for arresting photo generated holes of CdS. The analytical performance of the PEC analysis was related to the concentration

of AA in the test solution. As shown in Fig. S2A, the photocurrent could be much enhanced with increased concentration of added electron donor AA and reached a maximum for 0.1 M AA, then a decrease was observed for much higher concentrations of AA. As a hole scavenger, AA in lower concentrations would result in a fall in electrical output because fewer reducing agent molecules were available for electron donation to photogenerated holes. While a much higher concentration of AA would also result in the increase of the absorbance of AA in solution, as a consequence, the intensity of the irradiation arriving at the electrode surface decreased and the efficiency of excited CdS would decrease. Therefore, the optimal concentration of AA was set as 0.1 M. The pH is another key parameter that can affect the overall PEC signal, and it should also be optimized. As shown in Fig. S2B, the immunosensors were tested in a series of PBS with pH ranging from 5 to 8.5, the maximum photocurrent response appeared at pH of 7. Thus, pH 7 was chosen as the optimal pH value.

In this work, the concentration of Na_2S is also a key parameter that can affect the overall PEC signal, and it should also be optimized. Increasing the concentration could enhance the photocurrent. As shown in Fig. S2C, the photocurrent increased with the molarity from 0.1 to 0.7 M. In this work, 0.7 M of Na_2S, which is the biggest solubility, was chosen for the following experiments. The combination of specific interactions of antibody and antigen is another important factor that affects the photocurrent. With the increase of incubation time from 20 to 60 min, the immunosensor showed an increasing response until an incubation time of 50 min (Fig. S2D). Longer incubation time did not obviously improve the response. Therefore, the incubation time of 50 min was chosen as the optimal incubation time for the immunoassay of E_2.

3.4. Analytical performance

3.4.1. Calibration curve of estradiol

For the measurement of E_2, a competitive assay configuration was conducted under optimum conditions. A certain concentration of TiP@Cd^{2+}–Ab conjugates was mixed with the incubation solution containing a standard solution of estradiol with a series of known concentrations. The detection principle of the competitive immunization-based sensing platform as followings: the target E_2 in the solution competed with the immobilized E_2 on the electrode surface to bind the limited binding sites of the TiP@Cd^{2+}–Ab to form the immunocomplex. After addition of 0.7 M Na_2S and incubation for 30 min, CdS would be generated on the immunosensor surface due to the reaction between the S^{2-} and Cd^{2+}. After CdS was formed on the modified ITO electrodes, the photocurrent–time curve of the modified electrode was applied for the quantification of E_2. With the increase of target E_2 concentration, the amount of in situ generated CdS decreased and thus the photocurrent decreased. As presented in Fig. 3, the photocurrent changed linearly with the logarithm of E_2 concentration in the range from 5 pg/mL to 4 ng/mL with a correlation coefficient of 0.995. The detection limits was estimated to be 2 pg/mL ($S/N=3$), which was lower than the previous research (Li et al., 2013; Chaisuwan et al., 2013; Yildirim et al., 2012; Kim et al., 2007).

The analytical performance was also compared with the previous reports and our PEC sensor showed superiority over other methods in terms of both detection limit and dynamic range, as shown in Table S1 in the Supporting materials.

3.4.2. Reproducibility, stability and specificity

The reproducibility of the immunosensor was conducted by determining the estradiol with five sensors which were fabricated with the same procedure. Those five electrodes were used to detect the same concentration estradiol (1 ng/mL), a 3.8% of relative standard deviation (RSD) was obtained, indicating the good reproducibility of the immunosensor.

The selectivity of this system for E_2 at 1 ng/mL was evaluated over other common environmental endocrine, respectively, such as 100-fold 4-nnonylphenol (4NNP), estriol, as well as several other chemicals including 1-aminoanthraquinone, 2-methoxynaphthalene. As shown in Fig.4A, only the solution containing E_2 was obviously "Signal On", whereas the others remained nearly unchanged (the deviation ~5.0%).

Fig.4B showed the photocurrent responses of PEC sensor with the irradiation repeated every 10 s. The irradiation process was repeated 10 times over 300 s, during which time the photocurrent did not show any obvious change, which indicated that the photocurrent response was very stable and this strategy of in situ generated narrow-bandgap semiconductors was suitable for the construction of PEC sensors.

In order to evaluate the feasibility of the novel PEC sensor, we further tested the performance of the sensor in real samples by a standard addition method. In this study the localized lake water is adopted, the average recovery values were 104.7%~108.1% ($n=5$) obtained using the PEC sensor (Table 1), indicating the potential practicality of the PEC sensor for environmental samples with little interferences.

4. Conclusion

In this work, a novel PEC biosensor for estrodiol was proposed based on the in situ generated CdS-enhanced TiO_2film-based photoelectrochemistry via competitive strategy. An improved and quite simple method was used for in situ generation of CdS, and obviously, this assay is smart in design and easy in operation. Through the application of a competitive binding assay, the proposed biosensor showed a wide linear range of 5 pg/mL~4 ng/mL with a detection limit down to 2 pg/mL. This competitive, immunoreaction-based, PEC sensing platform integrated wide and narrow band elements into a collaborative detection method, which achieved a synergistic effect of high sensitivity, good specificity, simple operability, rapid response and acceptable stability. The results of practical application for E_2 in localized lake water were satisfactory. More than this, the strategy of employing in situ generated narrow-bandgap semiconductors to enhance the photocurrent opens up new avenues for PEC sensing.

Acknowledgments

This work was financially supported by the National Natural Science Foundation of China (Nos. 21375047, 21377046 and 21245007), the Science and Technology Plan Project of Jinan (No. 201307010), the Science and Technology Development Plan of Shandong Province (No. 2014GSF120004). QW thanks the Special Foundation for Taishan Scholar Professorship of Shandong Province and UJN (No. ts20130937).

Appendix A. Supplementary material

Supplementary data associated with this article can be found in the online version at http://dx.doi.org/10.1016/j.bios.2014.12.002.

References

Baker, D.R., Kamat, P.V., 2009. Adv. Funct. Mater. 19, 805–811.
Borgarello, E., Serpone, N., Grätzel, M., Pelizzetti, E., 1985. Int. J. Hydrog. Energy 10, 737–741.
Chang, H.-S., Choo, K.-H., Lee, B., Choi, S.-J., 2009. J. Hazard. Mater. 172, 1–12.

Chen, K., Liu, M., Zhao, G., Shi, H., Fan, L., Zhao, S., 2012a. Environ. Sci. Technol. 46, 11955–11961.
Chaisuwan, N., Xu, H., Wu, G., Liu, J., 2013. Biosens. Bioelectron. 46, 150–154.
Dong, D., Wang, F.-Q., Yang, X.-Q., Wang, N., Li, Y.-G., Guo, L.-H., Cheng, J., 2004. Anal. Chem. 76, 499–501.
Feng, L.-N., Peng, J., Zhu, Y.-D., Jiang, L.-P., Zhu, J.-J., 2012. Chem. Commun. 48, 4474–4476.
Gill, R., Zayats, M., Willner, I., 2008. Angew. Chem. Int. Ed. 47, 7602–7625.
Haddour, N., Chauvin, J., Gondran, C., Cosnier, S., 2006. J. Am. Chem. Soc. 128, 9693–9698.
Hintemann, T., Schneider, C., Schöler, H.F., Schneider, R.J., 2006. Water Res. 40, 2287–2294.
Hoffmann, M., Martin, S., Choi, W., Bahnemann, D., 1995. Chem. Rev. 95, 69–96.
Hosokawa, H., Fujiwara, H., Murakoshi, K., Wada, Y., Yanagida, S., Satoh, M., 1996. J. Phys. Chem. 100, 6649–6656.
Huang, Q., Tian, S., Zeng, D., Wang, X., Song, W., Li, Y., Xiao, W., Xie, C., 2013. ACS Catal. 3, 1477–1485.
Ikeda, A., Nakasu, M., Ogasawara, S., Nakanishi, H., Nakamura, M., Kikuchi, J.-i, 2009. Org. Lett. 11, 1163–1166.
Kim, Y.-S., Jung, H.-S., Matsuura, T., Lee, H.-Y., Kawai, T., Gu, M.-B., 2007. Biosens. Bioelectron. 22, 2525–2531.
Kim, H.-i, Kim, J., Kim, W., Choi, W., 2011. J. Phys. Chem. C 115, 9797–9805.
Li, H., Li, J., Xu, Q., Hu, X., 2011. Anal. Chem. 83, 9681–9686.
Li, J., Tu, W., Li, H., Bao, J., Dai, Z., 2014. Chem. Commun. 50, 2108–2110.
Li, Y.-J., Ma, M.-J., Yin, G., Kong, Y., Zhu, J.-J., 2013. Chem.-Eur. J. 19, 4496–4505.
Liang, M., Liu, S., Wei, M., Guo, L.-H., 2006. Anal. Chem. 78, 621–623.
Liang, M., Guo, L.-H., 2007. Environ. Sci. Technol. 41, 658–664.
Liang, Y., Kong, B., Zhu, A., Wang, Z., Tian, Y., 2011. Chem. Commun. 48, 245–247.
Lu, B., Liu, M., Shi, H., Huang, X., Zhao, G., 2013. Electroanalysis 25, 771–779.
Ma, W., Han, D., Gan, S., Zhang, N., Liu, S., Wu, T., Zhang, Q., Dong, X., Niu, L., 2013. Chem. Commun. 49, 7842–7844.
Pardo-Yissar, V., Katz, E., Wasserman, J., Willner, I., 2003. J. Am. Chem. Soc. 125, 622–623.
Qian, Z., Bai, H.-J., Wang, G.-L., Xu, J.-J., Chen, H.-Y., 2010. Biosens. Bioelectron 25, 2045–2050.
Sant, P.A., Kamat, P.V., 2002. PCCP 4, 198–203.
Shalom, M., Dor, S., Ruhle, S., Grinis, L., Zaban, A., 2009. J. Phys. Chem. C 113, 3895–3898.
Shen, Q., Zhao, X., Zhou, S., Hou, W., Zhu, J.-J., 2011. J. Phys. Chem. C 115, 17958–17964.
Shi, J., 2012. Chem. Rev. 113, 2139–2181.
Sun, B., Zhang, K., Chen, L., Guo, L., Ai, S., 2013. Biosens. Bioelectron. 44, 48–51.
Tambwekar, S., Venugopal, D., Subrahmanyam, M., 1999. Int. J. Hydrog. Energy 24, 957–963.
Tanaka, T., Takeda, H., Ueki, F., Obata, K., Tajima, H., Takeyama, H., Goda, Y., Fujimoto, S., Matsunaga, T., 2004. J. Biotechnol. 108, 153–159.
Tu, W., Dong, Y., Lei, J., Ju, H., 2010. Anal. Chem. 82, 8711–8716.
Wang, G.-L., Xu, J.-J., Chen, H.-Y., 2009a. Biosens. Bioelectron. 24, 2494–2498.
Wang, G.-L., Xu, J.-J., Chen, H.-Y., Fu, S.-Z., 2009b. Biosens. Bioelectron. 25, 791–796.
Wang, G.-L., Yu, P.-P., Xu, J.-J., Chen, H.-Y., 2009c. J. Phys. Chem. C 113, 11142–11148.
Wang, J.-y, Liu, Z.-h, Zheng, Q., He, Z.-k, Cai, R.-x, 2006. Nanotechnology 17, 4561.
Wen, Y., Zhou, B.-S., Xu, Y., Jin, S.-W., Feng, Y.-Q., 2006. J. Chromatogr. A 1133, 21–28.
Zhang, B., Guo, L.-H., Greenberg, M.M., 2012. Anal. Chem. 84, 6048–6053.
Yildirim, N., Long, F., Gao, C., He, M., Shi, H.-C., Gu, A.-Z., 2012. Environ. Sci. Technol. 46, 3288–3294.
Zhao, W.-W., Ma, Z.-Y., Yu, P.-P., Dong, X.-Y., Xu, J.-J., Chen, H.-Y., 2011. Anal. Chem. 84, 917–923.
Zhao, W.-W., Ma, Z.-Y., Yan, D.-Y., Xu, J.-J., Chen, H.-Y., 2012b. Anal. Chem. 84, 10518–10521.
Zhao, X., Zhou, S., Shen, Q., Jiang, L.-P., Zhu, J.-J., 2012c. Analyst 137, 3697–3703.